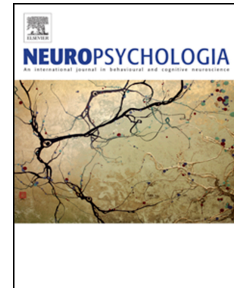


# Journal Pre-proof

Cortical thickness of primary visual cortex correlates with motion deficits in periventricular leukomalacia

Akshatha Bhat, Laura Biagi, Giovanni Cioni, Francesca Tinelli, M Concetta Morrone



PII: S0028-3932(20)30389-4

DOI: <https://doi.org/10.1016/j.neuropsychologia.2020.107717>

Reference: NSY 107717

To appear in: *Neuropsychologia*

Received Date: 27 April 2020

Revised Date: 27 November 2020

Accepted Date: 4 December 2020

Please cite this article as: Bhat, A., Biagi, L., Cioni, G., Tinelli, F., Morrone, M.C., Cortical thickness of primary visual cortex correlates with motion deficits in periventricular leukomalacia, *Neuropsychologia*, <https://doi.org/10.1016/j.neuropsychologia.2020.107717>.

This is a PDF file of an article that has undergone enhancements after acceptance, such as the addition of a cover page and metadata, and formatting for readability, but it is not yet the definitive version of record. This version will undergo additional copyediting, typesetting and review before it is published in its final form, but we are providing this version to give early visibility of the article. Please note that, during the production process, errors may be discovered which could affect the content, and all legal disclaimers that apply to the journal pertain.

© 2020 The Author(s). Published by Elsevier Ltd.

# Cortical thickness of primary visual cortex correlates with motion deficits in periventricular leukomalacia

Akshatha Bhat<sup>1,5</sup>, Laura Biagi<sup>4</sup>, Giovanni Cioni<sup>1,3</sup>, Francesca Tinelli<sup>1</sup>, M Concetta Morrone<sup>1,2</sup>

1-Department of Developmental Neuroscience, Laboratory of Vision, IRCCS Fondazione Stella Maris, Pisa, Italy

2-Department of Translational Research on New Technologies in Medicine and Surgery, University of Pisa, Italy

3-Department of Clinical and Experimental Medicine, University of Pisa, Italy

4-Laboratory of Medical Physics and Magnetic Resonance, IRCCS Fondazione Stella Maris, Pisa, Italy

5- Department of Neuroscience, University of Florence, Italy

## ABSTRACT

Impairments of visual motion perception and, in particular, of flow motion have been consistently observed in premature and very low birth weight subjects during infancy. Flow motion information is analyzed at various cortical levels along the dorsal pathways, with information mainly provided by primary and early visual cortex (V1, V2 and V3). We investigated the cortical stage of the visual processing that underlies these motion impairments, measuring Grey Matter Volume and Cortical Thickness in 13 children with Periventricular Leukomalacia (PVL). The cortical thickness, but not the grey matter volume of area V1, correlates negatively with motion coherence sensitivity, indicating that the thinner the cortex, the better the performance among the patients. However, we did not find any such association with either the thickness or volume of area MT, MST and areas of the IPS, suggesting damage at the level of primary visual cortex or along the optic radiation.

*Key words: cortical thickness, voxel-based morphometry, individual differences, MT, motion perception, PVL*

Journal Pre-proof

## 24 INTRODUCTION

25 Several cortical areas are identified as being involved in various levels of visual motion processing in humans.

26 The specialized areas for motion analysis are part of the visual dorsal pathways (Galletti & Fattori, 2018) and

27 among those areas MT, MST and V6/V6a play a major role in the analysis and perception of flow motion in humans

28 (O. J. Braddick, O'Brien, Wattam-Bell, Atkinson, & Turner, 2000; Cardin V, 2010; Gaglianese, et al., 2017;

29 Mikellidou, et al., 2018; Morrone, et al., 2000; Pitzalis, Sereno, et al., 2013; Tootell, Reppas, Dale, et al., 1995;

30 Tootell, Reppas, Kwong, et al., 1995; Zeki, et al., 1991). Activity of neurons in the MT and MST area varies linearly

31 with motion coherence (Rees, Friston, & Koch, 2000) and correlates with motion perception (Britten, Newsome,

32 Shadlen, Celebrini, & Movshon, 1996). The major visual input to the MT complex is provided by direct feedforward

33 from early cortical areas, like V1, V2 and V3. However many of the dorsal stream areas also receive direct thalamic

34 input (Bourne & Morrone, 2017; Bridge, Leopold, & Bourne, 2015) in primates and in humans, which becomes

35 important in mediating some form of perception in conditions of V1 lesion, like in blindsight (Ajina, Pestilli, Rokem,

36 Kennard, & Bridge, 2015; Weiskrantz, Warrington, Sanders, & Marshall, 1974). In typical children there is large

37 variability of flow motion sensitivity, only partially explained by a developmental trajectory, with structural cortical

38 areas contributing towards the large variability. In a large sample study, Braddick et al. (2016) examined

39 correlations of children's individual motion sensitivity with structural variations in different brain areas. The

40 authors found a strong correlation with Intraparietal areas, but not with MT, suggesting that, in children, the

41 limiting factor may be posed by the allocation of attention to motion signals. In addition, they observed a reduced

42 occipital lobe cortex, implying a front-end analysis of motion signals. We believe that the Braddick et al. (2016)

43 result calls for a new interpretation of the deficit of flow motion perception observed in many

44 neurodevelopmental disorders, from dyslexia to cerebral palsy, and that the origin of the deficit may arise from

45 disfunction of occipital cortical area and not necessarily of MT.

46 Deficits in visual motion perception (Birtles, Braddick, Wattam-Bell, Wilkinson, & Atkinson, 2007; Oliver Braddick,

47 Atkinson, & Wattam-Bell, 2003) have been consistently reported in the literature among premature and very low

48 birth weight subjects during infancy (for review see Atkinson, 2017; O. Braddick & Atkinson, 2011). Motion

49 perception deficits are widespread in premature groups, even where there is no direct evidence of brain lesions,

50 suggesting a high vulnerability of the dorsal pathway in prematurity. MacKay and colleagues (2005) have also  
51 shown that sensitivity to global motion perception (flow motion) was lower for preterm-born children both with  
52 and without periventricular damage, relative to term age-matched control (Atkinson & Braddick, 2007; Gunn, et  
53 al., 2002; Taylor NM, 2009). In particular, children with spastic diplegia and cystic PVL have, on average, impaired  
54 perception both for translational and rotational flow motion (Guzzetta, et al., 2009). However, there is great  
55 individual variability, with some patients having paradoxical and very specific abnormal perception. For example,  
56 we (Morrone, et al., 2008) observed PVL children with normal rotational or expansional motion perception of  
57 random dot kinematogram (RDK), who consistently reported the opposite direction of translating motion even at  
58 high coherence of the RDK, suggesting a malfunctioning of some basic mechanism of motion detectors. The  
59 inversion of perceived direction of motion was attributed to under-sampling of motion signals, which possibly may  
60 result from damage of the optic radiation itself, that provide the input to V1 direction selective neurons.

61 These peculiar deficits and the large variability observed suggest that the deficit in PVL may vary depending which  
62 particular pathway is affected by lesions along the optic radiation (Merabet, Mayer, Bauer, Wright, & Kran, 2017).  
63 In other words, in some subjects lesions of optic radiation may induce a generalized loss of peripheral magno-  
64 cellular pathways, in others the parvo-cellular pathway may be damaged resulting in agnosia, which is observed in  
65 some PVL children (Castaldi, Tinelli, Cicchini, & Morrone, 2018; Perez-Roche, et al., 2017) and, in others, optic  
66 radiation projecting to V1 may be totally spared but the lesions could affect the parallel bundles running more  
67 medially that project to MT and other dorsal motion areas. These different lesions would produce different  
68 perceptual deficits in the domain of motion.

69 While high resolution studies of optic tracts which could reveal small diffuse anatomical deficits, like in PVL, are  
70 difficult with present technologies, assessment of structural differences in the visual cortex are more feasible.  
71 Behavioral performance in visual functions have been often correlated with variation of surface, volume and  
72 thickness (Frank, Reavis, Greenlee, & Tse, 2016; Kanai & Rees, 2011) of the visual cortex. Here we investigated  
73 whether the poor sensitivity to global motion found in PVL children is associated with extrastriate areas such as  
74 MT+ and IPS or the primary cortical areas. Specifically, we investigated whether the grey matter volume or the

75 thickness of striate or extra striate areas predict the flow motion performance among patients with Periventricular  
 76 Leukomalacia.

## 77 METHODS

78 We selected 13 patients (mean  $\pm$  SD, aged  $11.2 \pm 4.5$  years, five males) from those referred to the Laboratory of  
 79 Vision of the Fondazione Stella Maris. The inclusion criteria were 1) clear signs of periventricular leukomalacia  
 80 (PVL) on perinatal brain ultrasounds and on MRI performed at later age, according to the criteria indicated in the  
 81 literature (Cioni, Bartalena, Biagioni, Boldrini, & Canapicchi, 1992) , 2) at least one brain MRI after 3 years of age,  
 82 3) good/normal or corrected-to-normal visual acuity, 4) absence of oculomotor dysfunctions and 5) good fixation  
 83 and no spontaneous nystagmus. The last inclusion criterion is essential to avoid artefactual impairment on visual  
 84 motion discrimination performance. Given the stringent selection criteria, we were able to select only 13 patients  
 85 from more than 130 in the follow up screening of the Laboratory of Vision. All selected patients were preterm with  
 86 gestational age less than 34 weeks, all had cerebral palsy (spastic diplegia); all had normal verbal IQ. A lesion  
 87 severity score was obtained for all subjects using a visual semi-quantitative scale for the classification of brain MRI,  
 88 specifically designed for individuals with cerebral palsy (Fiori, et al., 2014).

89 We also recruited 12 typical children between 7 and 11 years old, all with normal or corrected to normal vision to  
 90 compare with motion sensitivity of PVL patients.

Global score of Lesion

	age (y)	gender	Total	Right Hemisphere				Left Hemisphere				CC	Cereb
				R PV	R M	R CSC	R BG and BS	L PV	L M	L CSC	L BG and BS		
1	9	M	15.5	3.5	2.5	0	1	3.5	3	0	1	1	0
2	15	F	14.5	3.5	2	0	1	3.5	2.5	0	1	1	0
3	8	F	10.5	3.5	1.5	0	0	3.5	1	0	0	1	0
4	8	F	5.5	2	1.5	0	0	1	1	0	0	0	0
5	7	M	8.5	2.5	2	0	0	2.5	1.5	0	0	0	0
6	10	M	10	2.5	2	0	0	2.5	2	0	0	1	0
7	7	F	10	2.5	1	0	1	2.5	1	0	1	1	0
8	12	F	16.5	3.5	2.5	0	2	4	2.5	0	1	1	0
9	21	F	14	3.5	2.5	0	0	3.5	2.5	0	0	2	0
10	19	M	4.5	0.5	0.5	0	0	1.5	1	0	0	1	0
11	14	F	14.5	4	3	0	0	3.5	3	0	0	1	0
12	10	F	10.5	0	0	0	0	3.5	3	0	1	2	1
13	7	F	14.5	4	1.5	0	1	4	2	0	1	1	0

92 **Table 1. Demographical data and lesion severity scores for all patients.** The total score corresponds to the sum of  
93 raw scores of each hemisphere, subcortical structures (basal ganglia, BG, and brainstem, BS), corpus callosum (CC)  
94 and cerebellum (Cereb). For each hemisphere, the score is evaluated by considering a subdivision in three layers, a  
95 periventricular layer (PV), a middle white matter layer (M) and a cortico/subcortical layer (CSC).

96 The study was approved by the Ethics Committee of the Fondazione Stella Maris. Written informed consent for  
97 participation was obtained from all adult subjects and from the care providers of the children, in addition to verbal  
98 assent from the children.

99 Stimuli were presented to participants in a dimly lit room on a Sony CRT (17 inch) monitor with a mean luminance  
100 of 50 cd/m<sup>2</sup>, subtending 22x22 degrees when viewed from a distance of 57 cm. The tasks were run successively for  
101 each participant, with the order of presentation counterbalanced across participants. There were four to six  
102 training trials consisting of 100% coherent stimuli administered before the test trials to explain the task.

103 Stimuli comprised 100 small dots (each subtending 35 arc min), half black and half white. A proportion of the dots  
104 were caused to drift coherently at a local speed of 10 degrees/s (limited lifetime of five frames, frame rate 75 Hz),  
105 while the remaining dots (noise dots) were stationary (for five frames). At each frame 20% of dots were randomly  
106 assigned new positions, producing the appearance of dynamic flicker. The coherent motion was either clockwise or  
107 counter- clockwise (all dots had constant linear speed) for each trial. Participants were required to indicate the  
108 direction of the perceived motion pattern. Motion coherency of the stimuli was varied from trial-to-trial using the  
109 QUEST algorithm (Watson & Pelli, 1983) by substituting a proportion of the points with random noise. Sensitivity,  
110 defined as the inverse of the proportion of coherent dots producing 75% correct direction discrimination (Total  
111 Dots/ Coherent Dots), was calculated by fitting all data of a particular condition (at least 40 trials) with cumulative  
112 Gaussian functions.

113 Some of the PVL patients also participated in a previous experiment where motion and form sensitivity were  
114 assessed using the paradigm by Gunn et al. (2002). The noise dots in these tasks have the same speed of the  
115 coherent motion whilst, in our stimuli, noise dots are stationary. Table 2 reports the threshold of the 3 tasks

116 performance in z-score in order to compare the relative deficits. The normative data for the motion/form is taken  
117 from Gunn et al. (2002).

118

### 119 **Imaging Methods**

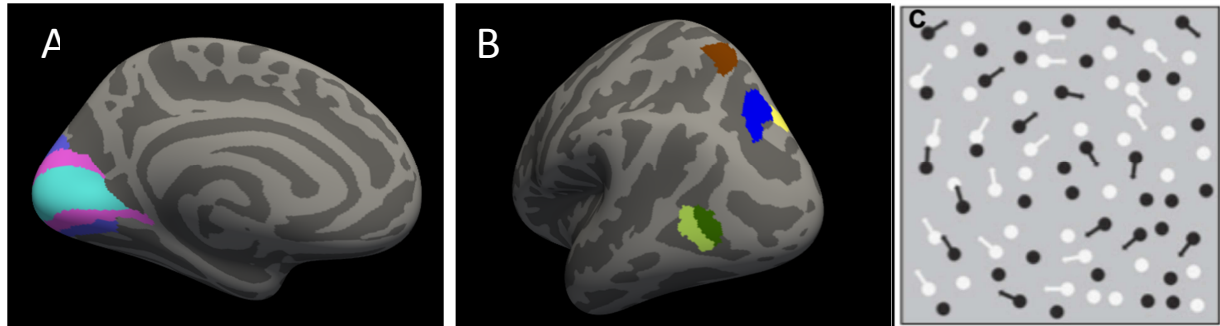
120 Imaging data were acquired on a GE 1.5 T HDx (General Electric Medical Systems) fitted with 40 mT/m high-speed  
121 gradients. The MRI session consisted of one structural session. A whole-brain fast spoiled gradient recalled  
122 acquisition T1-weighted series (3D BRAVO) was collected in the axial plane with Time of Repetition (TR)= 12.5 ms,  
123 Time of Echo (TE)=2.4 ms, Time of Inversion (TI)=450 ms, Flip Angle (FA)=13°, 1 mm slice thickness, in-plane  
124 resolution of 1mm.

125 **Pre-processing of anatomy:** All anatomies underwent a standard segmentation procedure using Freesurfer's  
126 *recon-all* command (Dale, Fischl, & Sereno, 1999), which produces white/grey matter segmentation and created  
127 meshes representing left and right hemisphere. Subject hemispheres were registered to the common template  
128 'fsaverage' to allow the registration of the regions-of-interest (ROIs) from the cortical template (Glasser, et al.,  
129 2016). We used HCP's multi-modal cortical parcellation atlas (Glasser, et al., 2016) which has detailed visual areas  
130 and has also been validated with retinotopy studies (Benson, et al., 2018)

131 **Definition of ROIs and Computing thickness:** Cortical ROIs were firstly projected onto the average anatomy  
132 'fsaverage' using the cortical template (Glasser, et al., 2016) and mapped back from 'fsaverage' space to the native  
133 cortical space using the *mri\_surf2surf* function. Cortical thickness was calculated as the distance between the  
134 white/ grey matter boundary and the pial surface (Dale, et al., 1999; Dickerson, et al., 2008). Reported cortical  
135 thicknesses for each ROI were the average across cerebral hemispheres within two bilateral ROIs.



136



137

138 **Figure 1. A, B: Locations of regions of interest (ROIs) on the inflated left hemisphere of an average brain.** The  
 139 medial view is depicted on the left side of the figure and the lateral view of the hemisphere is shown on the right  
 140 side. In Panel A, V1, V2 and V3 ROIs are illustrated in light-blue, magenta and blue respectively. In panel B Mt, MST,  
 141 V6A, IPS1 and VIP are illustrated in dark green, light green, yellow, blue and brown. All ROIs are obtained from the  
 142 HCP Glasses atlas (Glasser, et al., 2016). **C: Schematic diagram to illustrate the stimuli used to test circular  
 143 motion sensitivity.** The moving dots are illustrated by the vector and their proportion define motion coherence of  
 144 the stimulus.

145

#### 146 **Voxel Based Morphometry Analysis:**

147 The Voxel-based morphometry analysis was used to investigate the volume of the grey matter within the defined  
 148 ROIs, using the SPM12 package (Wellcome Trust Center for Neuroimaging, London, UK,  
 149 <http://www.fil.ion.ucl.ac.uk/spm/software/spm8/>) implemented in Matlab (Math Works, Natick, MA, USA). The T1-  
 150 weighted volumetric images were analyzed using the standard SPM pipeline with DARTEL algorithm to achieve an  
 151 accurate inter-subject registration with an improved realignment of small inner structures (Ashburner, 2007).  
 152 Standard steps were followed: (a) checking for scanner artifacts and gross anatomical abnormalities for each  
 153 subject; (b) setting the image origin to the anterior commissure; (c) segmenting the images into the GM and WM  
 154 images; (d) importing the parameter files produced by the tissue segmentation in the DARTEL procedure; (e) affine  
 155 transform of segmented brain maps into the MNI space (Ashburner, 2007); (f) modulation of segmented images  
 156 with the Jacobian determinants derived from the spatial normalization and (g) checking for homogeneity across  
 157 the sample and using standard smoothing by an 8-mm-full width-half maximum Gaussian kernel (Ashburner, 2007;  
 158 Good, et al., 2001). This preprocessing yielded the smoothed modulated normalized data in the MNI space, further  
 159 used for the volume count. Using the same ROIs defined for cortical thickness, total grey matter volume is

160 calculated, as estimated by the MATLAB *get\_totals.m* script implemented for SPM  
 161 ([http://www.sc.ucl.ac.uk/staff/g.ridgway/vbm/get\\_totals.m](http://www.sc.ucl.ac.uk/staff/g.ridgway/vbm/get_totals.m)). The grey matter volume of the individual subject is  
 162 scaled by the ratio between the overall brain volume of the subject and the overall average brain volume across all  
 163 subjects.

## 164 RESULTS

165 All 13 subjects were able to complete the psychophysical task with an average coherence sensitivity equal to 3.5  
 166 ( $0.54 \pm 0.07$  l.u.), corresponding to a mean threshold across subjects of 28% dots moving coherently. The average  
 167 sensitivity of typical children with age matched to the younger age group of PVL subjects is equal to 12 ( $1.1 \pm 0.08$   
 168 l.u.). These values are in line with previous reported data from the literature on PVL subjects and typical children  
 169 using the same stimuli (Guzzetta, et al., 2009). Table 2 reports the individual values and z-score for flow motion  
 170 measured in the present experiment and the z-score deficit for two other performances obtained from the form  
 171 and motion tasks used by Gunn et al. (2002). On average the deficit for our motion stimuli is similar to the motion  
 172 deficit by Gunn et al. (2002).

SUBJECT	Flow Sensitivity (L.u.)	Flow (z-score)	Form (z-score)	Motion (z-score)
S1	0.25	-2.9	-9.1	-7.3
S2	0.94	-0.4		
S3	0.28	-2.9	-3.2	-3.2
S4	0.88	-0.6	-3.2	0.0
S5	0.13	-3.4	-1.0	-1.8
S6	0.50	-2.0		
S7	0.49	-2.0		
S8	0.67	-1.4	-1.5	-1.0
S9	0.65	-1.5		
S10	0.78	-1.0	-0.5	0.0
S11	0.61	-1.6	-2.6	-0.4
S12	0.68	-1.4	-6.1	-2.8
S13	0.21	-3.1		
Mean	0.54	-1.9	-3.4	-2.1

173 **Table 2.** Comparisons of the z-score deficits between the flow motion task and form/motion tasks using the Gunn  
 174 et al. (2002) stimuli. The first column show the flow coherence sensitivity in logarithmic units

175 Subjects had a small impairment of visual acuity, on average  $0.08 \pm 0.03$  LogMAR. We found no significant  
176 correlation between Motion Sensitivity and Visual Acuity ( $p=0.091$ ,  $r= -0.49$ ,  $BF=0.87$ ) or with neuronal damage  
177 and only a marginally significant correlation of motion sensitivity with age ( $p=0.043$   $r=0.56$   $BF=1.6$ ), consistent with  
178 the previously reported maturation trajectory of motion discrimination (Atkinson, 2017; Hadad, Maurer, & Lewis,  
179 2011; Narasimhan S, 2012). In a preliminary analysis we performed a full brain grey matter correlation (Voxel-  
180 based morphometry analysis) with motion sensitivity, but we found no reliable correlation FDR for clusters greater  
181 than  $170 \text{ mm}^3$ . This was expected given that we were only able to recruit 13 subjects for the study, although we  
182 screened more than 130 potential patients with PVL. Given the small sample, we opted for a Region of Interest  
183 Analysis on major visual areas. We selected areas V1, V2, V3, MT, MST, V6a, IPS1 and VIP given that all these could  
184 be accurately located using the atlas currently available in visual science (Glasser, et al., 2016). We selected VIP  
185 because this area is close to the focus of the area correlation with motion sensitivity revealed by Braddick (2016)  
186 and corresponds to the focus of the non-symbolic number perception (Castaldi, Vignaud, & Eger, 2020); we  
187 selected V6a as an important area with direct input to MT/MST in the monkey (Pitzalis, Bozzacchi, et al., 2013;  
188 Pitzalis, Sereno, et al., 2013) and IPS1 as an intraparietal area related to attention (Szczepanski, Konen, & Kastner,  
189 2010). We tested whether the variability in perception of circular flow motion and visual acuity was associated  
190 with variability in brain structure by using two measures: cortical thickness and grey matter (GM) volume averaged  
191 across the ROIs. We also took into account age in the regression model.

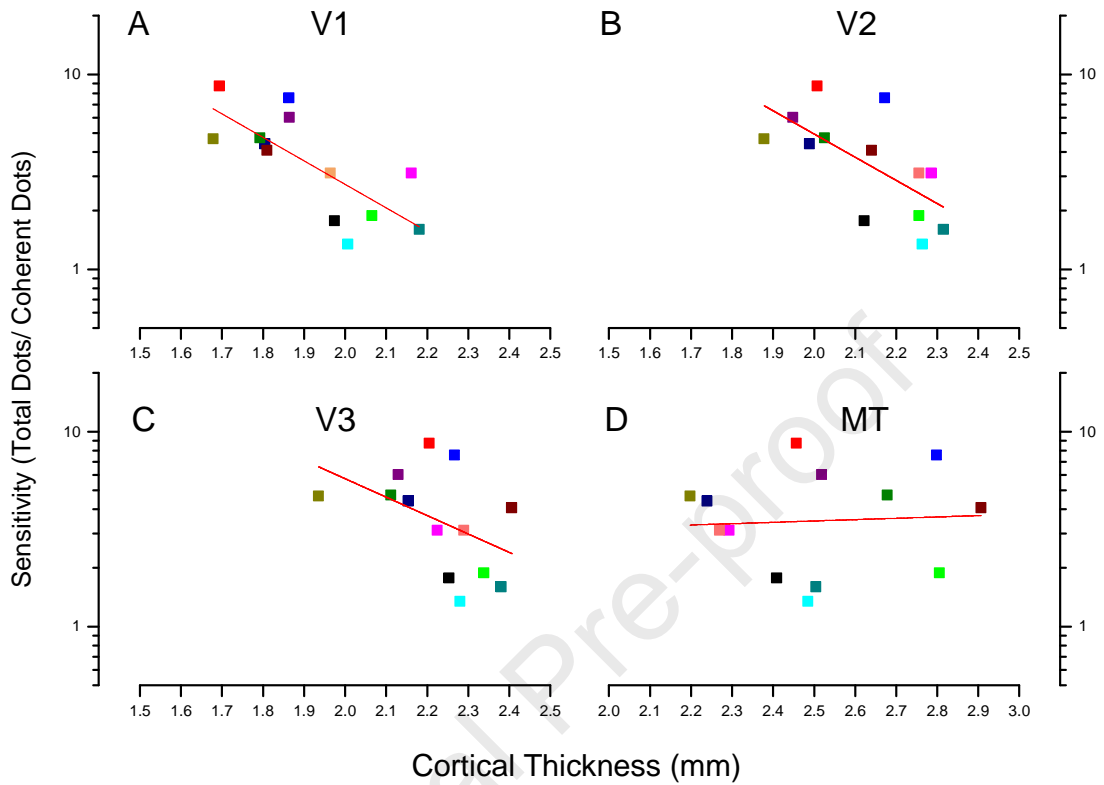
192 **Cortical Thickness:** Figure 2 shows the correlation of motion sensitivity with cortical thickness in areas V1, V2, V3  
193 and MT. The used ROIs are shown in figure 1 mapped onto the average brain. We found a significant negative  
194 correlation between cortical thickness and sensitivity for motion coherence in PVL patients in the bilateral visual  
195 area V1 ( $r = -0.75$ ,  $p = 0.001$ ,  $BF=15$ ) and bilateral V2 ( $r = -0.70$ ,  $p = 0.005$   $BA=4.9$ ) (Figure 2A,2B). The negative  
196 correlation with motion coherence sensitivity indicated that the thinner the cortex in these regions, the better the  
197 sensitivity of an individual. Interestingly, a non-significant trend for negative correlation is still present for area V3  
198 (Fig 2C,  $p=0.11$   $BF=0.7$ ), but is completely lost for areas MT (fig 2D) and MST (not shown) which both show a Bayes  
199 factor less than 0.3, indicating substantial evidence for the null hypothesis (random association between MT and  
200 MST and cortical thickness and sensitivity). A similar lack of significant correlation was evident for VIP and V6A,

201 two other important areas for cortical motion analysis, and for IPS1. All these areas showed a Bayes Factor below  
202 1.3 suggesting, if any, only marginal correlation. The lack of association of sensitivity with thickness of MT and the  
203 other motion sensitive areas is surprising.

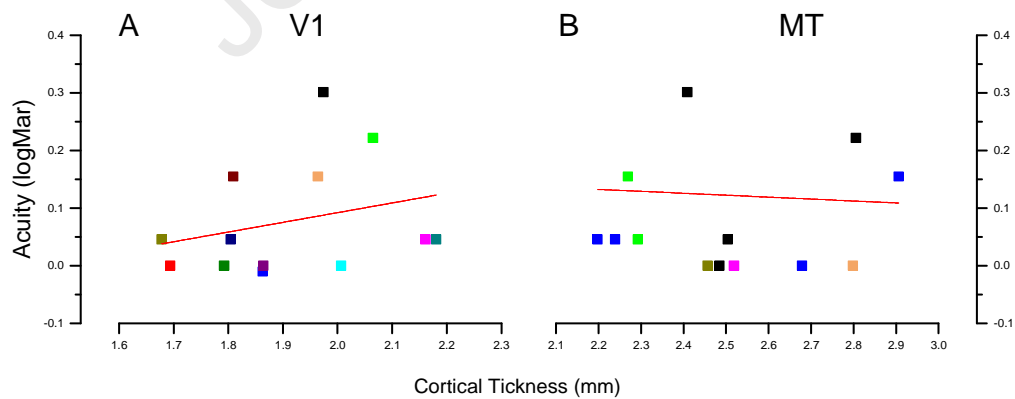
204 The age range of our PVL subjects was quite large, and cortical thickness in some associative areas continues to  
205 mature with age (Tamnes, et al., 2010). We did not find significant correlation of thickness parameters with the  
206 age of the patients for most areas, with the exception of a small trend of negative correlation for V1 ( $p=0.05$  and  
207  $BF=1.5$ ) and a robust and strong negative correlation for V2 ( $r=-0.72$ ,  $p=0.005$  and  $BF=12$ ) and IPS1 ( $r=-0.73$ ,  
208  $p=0.004$  and  $BF=12$ ). To determine whether the correlation with sensitivity was affected by age, we opted to  
209 compute partial correlation considering age as an additional regressor. Even the partial correlation results fail to  
210 provide an association of sensitivity with area MT, resulting in a  $r=0.2$  ( $p=0.6$ ;  $BF=0.2$ ), or with IPS1 ( $p=0.5$ ,  $BF=0.3$ )  
211 or V2 ( $p=0.15$ ,  $BF=0.6$ ). The same partial correlation procedure applied to V1 data, resulting in a Bayes factor of 3  
212 ( $r=-0.63$ ,  $p=0.028$ ), which confirmed a robust association between sensitivity and V1 thickness.

213 Thickness of areas V1 and V2 are highly positively correlated, ( $r = 0.87$ ,  $p = 0.0001$ ), less so with V3 ( $r=0.60$ ,  $p=0.03$ )  
214 and not at all with MT ( $r=0.02$ ,  $p=0.97$ ). Interestingly IPS1 thickness, which decreases strongly with age, is strongly  
215 correlated with V2 ( $BF=12$ ), weakly with V1, V3 and V6 ( $BF < 3$ ) and not at all with MT and MST. MT and MST  
216 thickness are highly correlated ( $r=0.74$ ,  $p=0.0037$ ,  $BF=13$ ).

217 We also considered whether visual acuity may be a good indicator of cortical thickness. Figure 3 shows the scatter  
218 plot of acuity (in LogMar) and thickness for V1 and MT. For both areas, the Bayes factor was around 0.2- 0.3,  
219 strongly suggesting the lack of association between the two parameters.



220  
 221 **Figure 2.** Correlation of cortical thickness of A: area V1, B: area V2, C: area V3 and D: area MT with patient's  
 222 sensitivity for motion coherence perception. Thickness values are the average values of the ROIs of the two  
 223 hemispheres. Different symbols correspond to the different subjects.



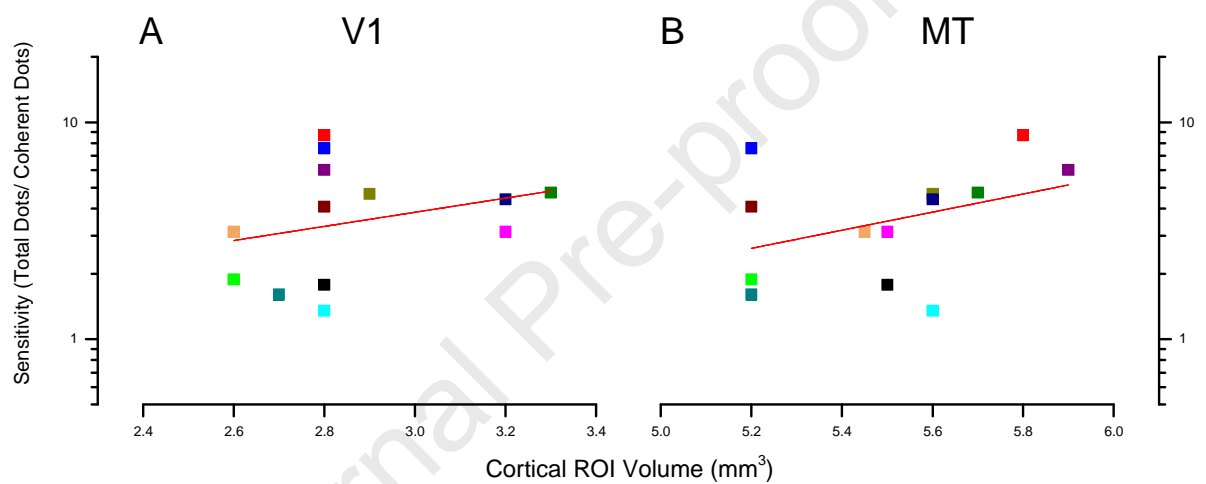
224  
 225 **Figure 3.** Correlation of cortical thickness of area V1 and MT with patient's visual acuity. All details as in figure 2

226

227

228 **Voxel-Based Morphometry:**

229 To cross-validate our findings, we conducted a voxel-based morphometry (VBM) analysis of GM density  
 230 (Ashburner, 2007) on the same data set and the same ROIs used in the thickness analysis. In this case, we did not  
 231 find significant correlations between GM volume and patients' motion coherence performance in early visual area  
 232 V1 ( $r = 0.29$ ,  $p = 0.31$ ), and in motion sensitive area MT+ ( $r = 0.39$ ,  $p = 0.16$ ). (Figure 4).



233

234

235 **Figure 4.** Correlation of Grey matter (GM) volume of A: area V1 and B: area MT+ with motion coherence sensitivity.  
 236 All details as in figure 2

237

## 238 DISCUSSION

239 These findings add to the scant literature of cortical thickness in cerebral palsy patients (Kelly, et al., 2015 ; Liu, et  
240 al., 2019; Pagnozzi, et al., 2020; Reid, et al., 2017). To the best of our knowledge, this is the first study exploring the  
241 association between anatomical differences and behavioral performance in visual functions among PVL  
242 populations. Our results demonstrate a strong negative correlation between sensitivity for motion coherence and  
243 primary visual cortex. Patients with thinner V1 were better at perceiving coherent motion at higher noise levels,  
244 while no such correlation was observed for the motion area MT, MST or other areas of the dorsal pathway. This  
245 result is surprising and suggests that the locus of the deficit is in V1 or earlier.

246 The lack of correlation in areas associated with dorsal pathways may contrast with the well-known selectivity of  
247 MT/MST, VIP and V6a motion (O. J. Braddick, et al., 2000; Cardin V, 2010; Gaglianese, et al., 2017; Mikellidou, et  
248 al., 2018; Morrone, et al., 2000; Pitzalis, Sereno, et al., 2013; Tootell, Reppas, Dale, et al., 1995; Tootell, Reppas,  
249 Kwong, et al., 1995; Zeki, et al., 1991) to coherent motion. It may also be considered not consistent with the  
250 correlation results between motion form detection and grey matter volume in IPS, demonstrated by Braddick et al.  
251 (2016), given that VIP ROI is anatomically included in the focus of the correlation. However, there are differences  
252 in the task and stimuli that may explain the different result. In our task the subject had to report the direction of  
253 the coherent motion integrated through all visual stimulus areas, while in Braddick et al. (2016) all subjects had to  
254 segment the form of a coherent flow from random direction noise of the same speed. This task is more complex  
255 and may require the analysis by higher motion area. In addition, in our stimuli noise dots were stationary and  
256 dynamically allocated at new positions every 70ms, generating a sense of dynamic flicker. In Braddick et al. (2016)  
257 the dots had the same speed as the coherent dots. V1 processing would not be able to detect the form by  
258 segmenting the motion signal, as we and others have demonstrated in BOLD experiments (O. J. Braddick, et al.,  
259 2000; Morrone, et al., 2000). The stimulus differences between experiments may shift the limiting factor for  
260 sensitivity from high to lower cortical area. The other major difference is the subject population. The limiting factor  
261 for sensitivity in typical children may be different from that in PVL. PVL is congenital, encompasses a non-focal  
262 white matter degeneration, and optic radiation is affected by the pathology (Groppo, et al., 2014). This anatomical  
263 evidence are consistent with early damage at the level of V1 innervation. In this light our result showing increased

264 V1 cortical thickness in PVL could provide an indirect but reliable measure of optic radiation damage that would be  
265 clinically more feasible to measure.

266 It is well known that the MT+ complex is functionally subdivided into the MT/TO1 area, which responds to  
267 contralateral visual motion stimulation, and the MST/TO2 area that responds to both ipsilateral and contralateral  
268 visual fields (Amano, Wandell, & Dumoulin, 2009; Huk, Dougherty, & Heeger, 2002; Morrone, et al., 2000). The two  
269 areas show the same BOLD selectivity to fast and slow motion (Mikellidou, et al., 2018), but a clear difference in  
270 selectivity for optic flow processing along complex trajectories such as spiral, expansion and rotational motion  
271 (Morrone, et al., 2000). Given that BOLD fMRI measures for MT+ can accurately estimate the underlying neuronal  
272 electrophysiological selectivity to motion, we might have expected a difference in the correlation with motion  
273 selectivity, if the limiting factor were located in this area. The fact that we observe no difference in correlation  
274 reinforces the idea of an earlier limiting factor. The thickness of MT and MST are highly correlated in PVL subjects,  
275 which poses difficulties in interpreting the lack of correlation of cortical thickness with perceptual motion  
276 discrimination. A direct BOLD motion response or direct ECoG registration would be more appropriate (Gaglianese,  
277 et al., 2017; Morrone, et al., 2008) to disentangle the different involvements of these area in PVL patients.

278 The result that the MT cortical thickness parameter did not correlate with motion sensitivity may be seen at odds  
279 with the current knowledge that MT processing limits our flow motion perception. However recent literature is  
280 converging with the idea that during development many of the properties of MT neurons are also determined by a  
281 direct subcortical thalamic input. In marmosets we know that this direct input, which normally would be pruned  
282 during typical development, becomes stabilized in presence of neonatal V1 lesion (Bourne & Morrone, 2017;  
283 Bridge, et al., 2015; Fox, Goodale, & Bourne, 2020; Warner CE, 2012). The shifting in the limiting factor in motion  
284 perception from MT to V1 in PVL patients might be consistent with a periventricular lesion that also affects this  
285 developing tract that connects LGN with MT. Tracts that connect dorsal visual area with LGN run more centrally  
286 and closer to the ventriculi than optic radiation projecting to V1 (Kurzawski, Mikellidou, Morrone, & Pestilli, 2020),  
287 reinforcing this idea. In future, it would be interesting to be able to address this question using high resolution DTI  
288 in human connectome in PVL patients.



289 The behavioral performance increases with age in our sample group ( $r = 0.53$ ,  $p = 0.03$ ). So thin visual areas  
290 correlating with the better performance could reflect (but also predict) the severity of damage of these congenital  
291 patients. However, the partial correlation analysis with age of the subjects as an additional regressor dismisses this  
292 criticism, given that the obtained Bayes Factor strongly supported the validity of a negative correlation of  
293 sensitivity with V1 thickness.

294 We did not observe any correlation with any performance parameters and volume analyzed with VBM. The  
295 differences between cortical thickness and VBM results could be due to a number of factors such as measurement  
296 of different aspects of GM structure. Interestingly, the literature suggests that these two parameters do not  
297 necessarily go hand in hand. A possible reason for the difference between the grey matter volume and the cortical  
298 thickness results is that, although cortical thickness changes can be detected in the volume measure, because  
299 volume is also dependent on surface area and therefore possibly cortical folding, it is less sensitive to specific  
300 changes in thickness compared with thickness measures (Hutton, Draganski, Ashburner, & Weiskopf, 2009). Hence,  
301 cortical thickness might be a more sensitive measurement to detect regional grey matter micro-changes that are  
302 missed by conventional voxel-based techniques at the earlier stages of the neurodegeneration due to partial  
303 volume effects (Hutton, et al., 2009; Seo, et al., 2012).

304 Anatomical developmental studies document monotonic thinning of cerebral cortex starting from the age of 4  
305 years (Brown, 2017; Fjell, et al., 2015; Parker, et al., 2020; Raznahan, et al., 2011; Sowell, et al., 2004; Thambisetty,  
306 et al., 2010; Vandekar, et al., 2015). Synaptic pruning, white matter encroachment on grey matter due to  
307 increasing axonal myelination, and changes in the extracellular matrix are assumed to underlie developmental  
308 changes and differences seen in grey matter volume between childhood and adulthood (Gogtay, et al., 2004;  
309 Gogtay & Thompson, 2010; Sowell, et al., 2004). Specifically, these structural changes may be related to more  
310 efficient and faster processing of information, which affects not only general intelligence, but also specific  
311 cognitive domains (Squeglia, Jacobus, Sorg, Jernigan, & Tapert, 2013). Elimination of unnecessary synaptic  
312 connections and increases in myelination could be contributing to the observed results in the above-mentioned  
313 studies. All these maturation processes are impaired during the development of preterm children (Volpe, 2009a,  
314 2009b). PVL is characterized by lesions to the cerebral white matter, usually occurring between the 24th and 36th

315 week of gestational age. There is often observed deficiency of fully differentiated oligodendrocytes and hypo-  
316 myelination with dilated ventricles (Cheong, et al., 2009; Volpe, 2009a). As it is with the healthy developing  
317 population (Song, Schwarzkopf, Kanai, & Rees, 2015), we show that in PVL thinner cortex is also associated with  
318 better visual performance. The alternative explanation of the negative correlation of V1 thickness and motion  
319 sensitivity may be formulated by considering cross-modal plasticity. Congenitally blind subjects have thicker V1,  
320 probably reflecting the reorganization of V1 circuitry to process other sensory inputs (Jiang, et al., 2009; Park, et  
321 al., 2009). A partially deafferented V1, as a consequence of optic radiation lesion in PVL newborns, should  
322 plastically rearrange to process other sensory inputs and hence become thicker than in normal controls. A  
323 comparison between two blind children with and without PVL shows decreased white matter connections,  
324 particularly in the occipital pole (Merabet, et al., 2017), supporting an altered input to V1 in PVL.

325  
326 It is interesting that visual acuity (VA) deficits do not correlate with any anatomical measures. It is well known in  
327 the clinical practice that VA is not a good predictor of PVL disabilities. Indeed, many PVL patients, despite having  
328 good oculomotor control and normal VA, can have profound alteration of vision. Many have agnosia, for faces  
329 (Perez-Roche, et al., 2017), and objects but also for simple features like orientation or symmetry (Castaldi, et al.,  
330 2018) . Others have alteration more specific for the dorsal pathways, like the motion perceptual deficit observed  
331 here. However, even within the population with only altered motion perception, there are a wide variety of  
332 deficits, some very peculiar like the reliable perception of the inverse direction of motion (Morrone, et al., 2008).  
333 As suggested in the study of these patients, the deficit may be traced to specific pathways of the optic radiation.  
334 Magnocellular pathways of the optic radiation are more sensitive to compression damage than parvocellular  
335 pathways, having a larger diameter of the axons. It is possible that, in many patients, the compression reduced the  
336 density of the magnocellular input to V1, inducing a reduction of the flow motion sensitivity and, in extreme cases,  
337 the reduction is so pronounced to induce under-sampling of motion and, hence, the perception of inverse  
338 direction in special circumstances. This is consistent with the finding of unimpaired visual acuity of the patients  
339 that it is mediated mainly by the parvocellular pathway, especially for foveal targets.

340 Given the importance of understanding the reorganization of the motion pathway in the PVL children, it is  
341 suggested that more patients should be tested in flow motion in future. Unfortunately, we were only able to

342 recruit 13 patients given the stringent criteria and in particular the need to have an MRI after 5 years of age,  
343 despite having screened more than 130 PVL patient records. Although the sample is small, it was crucial to avoid  
344 artefactual data collection due to abnormal eye movements that can greatly impact on motion perception.  
345 However, having demonstrated in this clean sample that the correlation of sensitivity with V1 is very strong, as  
346 suggested by a Bayes Factor of 15, we hope in future to relax our selection criteria and extend the analysis to a  
347 much larger population. If successful, we might also be able to define the thickness of calcarine sulcus as a clinical  
348 predictor of visual ability.

349 Our results contribute to the developmental literature which, so far, demonstrates that thinner cortices relate to  
350 better global cognitive functioning, as well as improved functioning in domain-specific tasks (Squeglia, et al., 2013).  
351 Any irregularities to typical thinning during neurodegenerative diseases, traumatic brain injury, or medical illness  
352 could have implications on later expected perceptual and behavioral functioning. Future research with a larger  
353 sample size using longitudinal data will shed light on the effect of cortical thinning on visual and other high-level  
354 functioning in the congenital patient population.

## 355 ACKNOWLEDGMENT

356 This research was supported by the European Research Council under the European Union's (H2020) - ERC  
357 Advanced "Spatio-temporal mechanisms of generative perception" Grant N. 832813 — GenPercept (M.C.M.) and  
358 by the European Union's Horizon 2020 Research and Innovation Programme under the Marie Skłodowska-Curie  
359 grant agreement number 641805 (A.B.), by the Italian Ministry of University and Research under the project  
360 PRIN2017 (M.C.M) and Italian Ministry of Health 2017.

361

362

363

364

365

## 366 REFERENCES

- 367 Ajina, S., Pestilli, F., Rokem, A., Kennard, C., & Bridge, H. (2015). Human blindsight is mediated by an intact  
368 geniculo-extrastriate pathway. *Elife*, *4*.
- 369 Ashburner, J. (2007). A fast diffeomorphic image registration algorithm. *Neuroimage*, *38*, 95-113.
- 370 Atkinson, J. (2017). The Davida Teller Award Lecture, 2016: Visual Brain Development: A review of "Dorsal Stream  
371 Vulnerability"-motion, mathematics, amblyopia, actions, and attention. *J Vis*, *17*, 26.
- 372 Atkinson, J., & Braddick, O. (2007). Visual and visuocognitive development in children born very prematurely. *Prog*  
373 *Brain Res*, *164*, 123-149.
- 374 Benson, N. C., Jamison, K. W., Arcaro, M. J., Vu, A. T., Glasser, M. F., Coalson, T. S., Van Essen, D. C., Yacoub, E.,  
375 Ugurbil, K., Winawer, J., & Kay, K. (2018). The Human Connectome Project 7 Tesla retinotopy dataset:  
376 Description and population receptive field analysis. *J Vis*, *18*, 23.
- 377 Birtles, D. B., Braddick, O. J., Wattam-Bell, J., Wilkinson, A. R., & Atkinson, J. (2007). Orientation and motion-  
378 specific visual cortex responses in infants born preterm. *Neuroreport*, *18*, 1975-1979.
- 379 Bourne, J. A., & Morrone, M. C. (2017). Plasticity of Visual Pathways and Function in the Developing Brain: Is the  
380 Pulvinar a Crucial Player? *Front Syst Neurosci*, *11*, 3.
- 381 Braddick, O., & Atkinson, J. (2011). Development of human visual function. *Vision Res*, *51*, 1588-1609.
- 382 Braddick, O., Atkinson, J., Newman, E., Akshoomoff, N., Kuperman, J. M., Bartsch, H., Chen, C. H., Dale, A. M., &  
383 Jernigan, T. L. (2016). Global Visual Motion Sensitivity: Associations with Parietal Area and Children's  
384 Mathematical Cognition. *J Cogn Neurosci*, *28*, 1897-1908.
- 385 Braddick, O., Atkinson, J., & Wattam-Bell, J. (2003). Normal and anomalous development of visual motion  
386 processing: motion coherence and 'dorsal-stream vulnerability'. *Neuropsychologia*, *41*, 1769-1784.
- 387 Braddick, O. J., O'Brien, J. M., Wattam-Bell, J., Atkinson, J., & Turner, R. (2000). Form and motion coherence  
388 activate independent, but not dorsal/ventral segregated, networks in the human brain. *Curr Biol*, *10*, 731-  
389 734.
- 390 Bridge, H., Leopold, D. A., & Bourne, J. A. (2015). Adaptive Pulvinar Circuitry Supports Visual Cognition. *Trends*  
391 *Cogn Sci*.
- 392 Britten, K. H., Newsome, W. T., Shadlen, M. N., Celebrini, S., & Movshon, J. A. (1996). A relationship between  
393 behavioral choice and the visual responses of neurons in macaque MT. *Vis Neurosci*, *13*, 87-100.
- 394 Brown, T. T. (2017). Individual differences in human brain development. *Wiley Interdiscip Rev Cogn Sci*, *8*.
- 395 Cardin V, S. A. (2010). Sensitivity of Human Visual and Vestibular Cortical Regions to Egomotion-Compatible Visual  
396 Stimulation. *Cerebral Cortex*, *20*, 1964--1973.
- 397 Castaldi, E., Tinelli, F., Cicchini, G. M., & Morrone, M. C. (2018). Supramodal agnosia for oblique mirror orientation  
398 in patients with periventricular leukomalacia. *Cortex*, *103*, 179-198.
- 399 Castaldi, E., Vignaud, A., & Eger, E. (2020). Mapping subcomponents of numerical cognition in relation to functional  
400 and anatomical landmarks of human parietal cortex. *Neuroimage*, *221*, 117210.
- 401 Cheong, J. L., Thompson, D. K., Wang, H. X., Hunt, R. W., Anderson, P. J., Inder, T. E., & Doyle, L. W. (2009).  
402 Abnormal white matter signal on MR imaging is related to abnormal tissue microstructure. *AJNR Am J*  
403 *Neuroradiol*, *30*, 623-628.
- 404 Cioni, G., Bartalena, L., Biagioni, E., Boldrini, A., & Canapicchi, R. (1992). Neuroimaging and functional outcome of  
405 neonatal leukomalacia. *Behav Brain Res*, *49*, 7-19.
- 406 Dale, A. M., Fischl, B., & Sereno, M. I. (1999). Cortical surface-based analysis. I. Segmentation and surface  
407 reconstruction. *Neuroimage*, *9*, 179-194.
- 408 Dickerson, B. C., Fenstermacher, E., Salat, D. H., Wolk, D. A., Maguire, R. P., Desikan, R., Pacheco, J., Quinn, B. T.,  
409 Van der Kouwe, A., Greve, D. N., Blacker, D., Albert, M. S., Killiany, R. J., & Fischl, B. (2008). Detection of  
410 cortical thickness correlates of cognitive performance: Reliability across MRI scan sessions, scanners, and  
411 field strengths. *Neuroimage*, *39*, 10-18.

- 412 Fiori, S., Cioni, G., Klingels, K., Ortibus, E., Van Gestel, L., Rose, S., Boyd, R. N., Feys, H., & Guzzetta, A. (2014).  
 413 Reliability of a novel, semi-quantitative scale for classification of structural brain magnetic resonance  
 414 imaging in children with cerebral palsy. *Dev Med Child Neurol*, *56*, 839-845.
- 415 Fjell, A. M., Grydeland, H., Krogsrud, S. K., Amlien, I., Rohani, D. A., Ferschlmann, L., Storsve, A. B., Tamnes, C. K.,  
 416 Sala-Llonch, R., Due-Tønnessen, P., Bjørnerud, A., Solsnes, A. E., Haberg, A. K., Skranes, J., Bartsch, H.,  
 417 Chen, C. H., Thompson, W. K., Panizzon, M. S., Kremen, W. S., Dale, A. M., & Walhovd, K. B. (2015).  
 418 Development and aging of cortical thickness correspond to genetic organization patterns. *Proc Natl Acad Sci U S A*, *112*, 15462-15467.
- 420 Fox, D. M., Goodale, M. A., & Bourne, J. A. (2020). The Age-Dependent Neural Substrates of Blindsight. *Trends*  
 421 *Neurosci*, *43*, 242-252.
- 422 Frank, S. M., Reavis, E. A., Greenlee, M. W., & Tse, P. U. (2016). Pretraining Cortical Thickness Predicts Subsequent  
 423 Perceptual Learning Rate in a Visual Search Task. *Cereb Cortex*, *26*, 1211-1220.
- 424 Gaglianese, A., Vansteensel, M. J., Harvey, B. M., Dumoulin, S. O., Petridou, N., & Ramsey, N. F. (2017).  
 425 Correspondence between fMRI and electrophysiology during visual motion processing in human MT.  
 426 *Neuroimage*, *155*, 480-489.
- 427 Galletti, C., & Fattori, P. (2018). The dorsal visual stream revisited: Stable circuits or dynamic pathways? *Cortex*, *98*,  
 428 203-217.
- 429 Glasser, M. F., Coalson, T. S., Robinson, E. C., Hacker, C. D., Harwell, J., Yacoub, E., Ugurbil, K., Andersson, J.,  
 430 Beckmann, C. F., Jenkinson, M., Smith, S. M., & Van Essen, D. C. (2016). A multi-modal parcellation of  
 431 human cerebral cortex. *Nature*, *536*, 171-178.
- 432 Gogtay, N., Giedd, J. N., Lusk, L., Hayashi, K. M., Greenstein, D., Vaituzis, A. C., Nugent, T. F., 3rd, Herman, D. H.,  
 433 Clasen, L. S., Toga, A. W., Rapoport, J. L., & Thompson, P. M. (2004). Dynamic mapping of human cortical  
 434 development during childhood through early adulthood. *Proc Natl Acad Sci U S A*, *101*, 8174-8179.
- 435 Gogtay, N., & Thompson, P. M. (2010). Mapping gray matter development: implications for typical development  
 436 and vulnerability to psychopathology. *Brain Cogn*, *72*, 6-15.
- 437 Good, C. D., Johnsrude, I. S., Ashburner, J., Henson, R. N., Friston, K. J., & Frackowiak, R. S. (2001). A voxel-based  
 438 morphometric study of ageing in 465 normal adult human brains. *Neuroimage*, *14*, 21-36.
- 439 Groppo, M., Ricci, D., Bassi, L., Merchant, N., Doria, V., Arichi, T., Allsop, J. M., Ramenghi, L., Fox, M. J., Cowan, F.  
 440 M., Counsell, S. J., & Edwards, A. D. (2014). Development of the optic radiations and visual function after  
 441 premature birth. *Cortex*, *56*, 30-37.
- 442 Gunn, A., Cory, E., Atkinson, J., Braddick, O., Wattam-Bell, J., Guzzetta, A., & Cioni, G. (2002). Dorsal and ventral  
 443 stream sensitivity in normal development and hemiplegia. In *Neuroreport* (2002/05/09 ed., Vol. 13, pp.  
 444 843-847).
- 445 Guzzetta, A., Tinelli, F., Del Viva, M. M., Bancale, A., Arrighi, R., Pascale, R. R., & Cioni, G. (2009). Motion perception  
 446 in preterm children: role of prematurity and brain damage. *Neuroreport*, *20*, 1339-1343.
- 447 Hadad, B. S., Maurer, D., & Lewis, T. L. (2011). Long trajectory for the development of sensitivity to global and  
 448 biological motion. *Dev Sci*, *14*, 1330-1339.
- 449 Hutton, C., Draganski, B., Ashburner, J., & Weiskopf, N. (2009). A comparison between voxel-based cortical  
 450 thickness and voxel-based morphometry in normal aging. *Neuroimage*, *48*, 371-380.
- 451 Jiang, J., Zhu, W., Shi, F., Liu, Y., Li, J., Qin, W., Li, K., Yu, C., & Jiang, T. (2009). Thick visual cortex in the early blind. *J*  
 452 *Neurosci*, *29*, 2205-2211.
- 453 Kanai, R., & Rees, G. (2011). The structural basis of inter-individual differences in human behaviour and cognition.  
 454 *Nat Rev Neurosci*, *12*, 231-242.
- 455 Kelly, C. E., Chan, L., Burnett, A. C., Lee, K. J., Connelly, A., Anderson, P. J., Doyle, L. W., Cheong, J. L., Thompson, D.  
 456 K., & Victorian Infant Collaborative Study, G. (2015). Brain structural and microstructural alterations  
 457 associated with cerebral palsy and motor impairments in adolescents born extremely preterm and/or  
 458 extremely low birthweight. *Dev Med Child Neurol*, *57*, 1168-1175.
- 459 Kurzwaski, J. W., Mikellidou, K., Morrone, M. C., & Pestilli, F. (2020). The visual white matter connecting human  
 460 area prostriata and the thalamus is retinotopically organized. *Brain Struct Funct*, *225*, 1839-1853.
- 461 Liu, H., Jiang, H., Bi, W., Huang, B., Li, X., Wang, M., Wang, X., Zhao, H., Cheng, Y., Tao, X., Liu, C., Huang, T., Jin, C.,  
 462 Zhang, T., & Yang, J. (2019). Abnormal Gray Matter Structural Covariance Networks in Children With  
 463 Bilateral Cerebral Palsy. *Front Hum Neurosci*, *13*, 343.

- 464 MacKay, T. L., Jakobson, L. S., Ellemberg, D., Lewis, T. L., Maurer, D., & Casiro, O. (2005). Deficits in the processing  
465 of local and global motion in very low birthweight children. *Neuropsychologia*, *43*, 1738-1748.
- 466 Merabet, L. B., Mayer, D. L., Bauer, C. M., Wright, D., & Kran, B. S. (2017). Disentangling How the Brain is "Wired"  
467 in Cortical (Cerebral) Visual Impairment. *Semin Pediatr Neurol*, *24*, 83-91.
- 468 Mikellidou, K., Frijia, F., Montanaro, D., Greco, V., Burr, D. C., & Morrone, M. C. (2018). Cortical BOLD responses to  
469 moderate- and high-speed motion in the human visual cortex. *Sci Rep*, *8*, 8357.
- 470 Morrone, M., Guzzetta, A., Tinelli, F., Tosetti, M., Del Viva, M., Montanaro, D., Burr, D. C., & Cioni, G. (2008).  
471 Inversion of Perceived Direction of Motion Caused by Spatial Undersampling in Two Children with  
472 Periventricular Leukomalacia. *Journal of Cognitive Neuroscience*, *20*, 1094–1106.
- 473 Morrone, M., Tosetti, M., Montanaro, D., Fiorentini, A., Cioni, G., & Burr, D. (2000). A cortical area that responds  
474 specifically to optic flow, revealed by fMRI. *Nature Neuroscience* *3*, 1322-1328.
- 475 Narasimhan S, G. D. (2012). The effect of dot speed and density on the development of global motion perception.  
476 *Vision Research* *62*, 102–107.
- 477 Pagnozzi, A. M., Pannek, K., Fripp, J., Fiori, S., Boyd, R. N., & Rose, S. (2020). Understanding the impact of bilateral  
478 brain injury in children with unilateral cerebral palsy. *Hum Brain Mapp*.
- 479 Park, H. J., Lee, J. D., Kim, E. Y., Park, B., Oh, M. K., Lee, S., & Kim, J. J. (2009). Morphological alterations in the  
480 congenital blind based on the analysis of cortical thickness and surface area. *Neuroimage*, *47*, 98-106.
- 481 Parker, N., Patel, Y., Jackowski, A. P., Pan, P. M., Salum, G. A., Pausova, Z., Paus, T., Saguenay Youth, S., & the, I. C.  
482 (2020). Assessment of Neurobiological Mechanisms of Cortical Thinning During Childhood and  
483 Adolescence and Their Implications for Psychiatric Disorders. *JAMA Psychiatry*.
- 484 Perez-Roche, T., Altemir, I., Gimenez, G., Prieto, E., Gonzalez, I., Lopez Pison, J., & Pueyo, V. (2017). Face  
485 recognition impairment in small for gestational age and preterm children. *Res Dev Disabil*, *62*, 166-173.
- 486 Pitzalis, S., Bozzacchi, C., Bultrini, A., Fattori, P., Galletti, C., & Di Russo, F. (2013). Parallel motion signals to the  
487 medial and lateral motion areas V6 and MT+. *Neuroimage*, *67*, 89-100.
- 488 Pitzalis, S., Sereno, M. I., Committeri, G., Fattori, P., Galati, G., Tosoni, A., & Galletti, C. (2013). The human  
489 homologue of macaque area V6A. *Neuroimage*, *82*, 517-530.
- 490 Raznahan, A., Shaw, P., Lalonde, F., Stockman, M., Wallace, G. L., Greenstein, D., Clasen, L., Gogtay, N., & Giedd, J.  
491 N. (2011). How does your cortex grow? *J Neurosci*, *31*, 7174-7177.
- 492 Rees, G., Friston, K., & Koch, C. (2000). A direct quantitative relationship between the functional properties of  
493 human and macaque V5. *Nat Neurosci*, *3*, 716-723.
- 494 Reid, L. B., Pagnozzi, A. M., Fiori, S., Boyd, R. N., Dowson, N., & Rose, S. E. (2017). Measuring neuroplasticity  
495 associated with cerebral palsy rehabilitation: An MRI based power analysis. *Int J Dev Neurosci*, *58*, 17-25.
- 496 Seo, S. W., Lee, J. M., Im, K., Park, J. S., Kim, S. H., Kim, S. T., Ahn, H. J., Chin, J., Cheong, H. K., Weiner, M. W., & Na,  
497 D. L. (2012). Cortical thinning related to periventricular and deep white matter hyperintensities. *Neurobiol*  
498 *Aging*, *33*, 1156-1167.
- 499 Song, C., Schwarzkopf, D. S., Kanai, R., & Rees, G. (2015). Neural population tuning links visual cortical anatomy to  
500 human visual perception. *Neuron*, *85*, 641-656.
- 501 Sowell, E. R., Thompson, P. M., Leonard, C. M., Welcome, S. E., Kan, E., & Toga, A. W. (2004). Longitudinal mapping  
502 of cortical thickness and brain growth in normal children. *J Neurosci*, *24*, 8223-8231.
- 503 Squeglia, L. M., Jacobus, J., Sorg, S. F., Jernigan, T. L., & Tapert, S. F. (2013). Early adolescent cortical thinning is  
504 related to better neuropsychological performance. *J Int Neuropsychol Soc*, *19*, 962-970.
- 505 Szczepanski, S. M., Konen, C. S., & Kastner, S. (2010). Mechanisms of spatial attention control in frontal and  
506 parietal cortex. *J Neurosci*, *30*, 148-160.
- 507 Tamnes, C. K., Ostby, Y., Fjell, A. M., Westlye, L. T., Due-Tonnessen, P., & Walhovd, K. B. (2010). Brain maturation in  
508 adolescence and young adulthood: regional age-related changes in cortical thickness and white matter  
509 volume and microstructure. *Cereb Cortex*, *20*, 534-548.
- 510 Taylor NM, J. L., Maurer D, Lewis TL. (2009). Differential vulnerability of global motion, global form, and biological  
511 motion processing in full-term and preterm children. *Neuropsychologia*, *47*, 2766–2778.
- 512 Thambisetty, M., Wan, J., Carass, A., An, Y., Prince, J. L., & Resnick, S. M. (2010). Longitudinal changes in cortical  
513 thickness associated with normal aging. *Neuroimage*, *52*, 1215-1223.
- 514 Tootell, R. B., Reppas, J. B., Dale, A. M., Look, R. B., Sereno, M. I., Malach, R., Brady, T. J., & Rosen, B. R. (1995).  
515 Visual motion aftereffect in human cortical area MT revealed by functional magnetic resonance imaging.  
516 *Nature*, *375*, 139-141.

- 517 Tootell, R. B., Reppas, J. B., Kwong, K. K., Malach, R., Born, R. T., Brady, T. J., Rosen, B. R., & Belliveau, J. W. (1995).  
518 Functional analysis of human MT and related visual cortical areas using magnetic resonance imaging. *J*  
519 *Neurosci*, *15*, 3215-3230.
- 520 Vandekar, S. N., Shinohara, R. T., Raznahan, A., Roalf, D. R., Ross, M., DeLeo, N., Ruparel, K., Verma, R., Wolf, D. H.,  
521 Gur, R. C., Gur, R. E., & Satterthwaite, T. D. (2015). Topologically dissociable patterns of development of  
522 the human cerebral cortex. *J Neurosci*, *35*, 599-609.
- 523 Volpe, J. J. (2009a). Brain injury in premature infants: a complex amalgam of destructive and developmental  
524 disturbances. *Lancet Neurol*, *8*, 110-124.
- 525 Volpe, J. J. (2009b). The encephalopathy of prematurity--brain injury and impaired brain development inextricably  
526 intertwined. *Semin Pediatr Neurol*, *16*, 167-178.
- 527 Warner CE, K. W., BourneJA. (2012). The Early Maturation of Visual Cortical Area MT is Dependent on Input from  
528 the Retinorecipient Medial Portion of the Inferior Pulvinar. *The Journal of Neuroscience*, *32*, 17073-17085.
- 529 Weiskrantz, L., Warrington, E. K., Sanders, M. D., & Marshall, J. (1974). Visual capacity in the hemianopic field  
530 following a restricted occipital ablation. *Brain*, *97*, 709-728.
- 531 Zeki, S., Watson, J. D., Lueck, C. J., Friston, K. J., Kennard, C., & Frackowiak, R. S. (1991). A direct demonstration of  
532 functional specialization in human visual cortex. *J Neurosci*, *11*, 641-649.

533

In this manuscript we present evidence of a reliable correlation between Cortical Thickness of primary visual cortex and Flow Motion Sensitivity in PVL patients.

Journal Pre-proof